NUMERICAL ANALYSIS ON EFFECT OF STEEL PIPE SHEET PILE REINFORCEMENT TO CAISSON FOUNDATION

Koichi Isobe[i], Makoto Kimura[ii], Feng Zhang[iii], Koichiro Danno[i]
Kenji Kohno[iv], Noriyoshi Harata[iv], Takeshi Makino [iv], Takeshi Kuwajima [iv]

ABSTRACT

In this paper, centrifugal model tests and three dimensional elasto-plastic finite element method analyses are conducted to investigate the mechanical behavior of the caisson foundation systems reinforced by steel pipe sheet piles (SPSP). Main attention is paid to the following factors that may affect the effect of SPSP reinforcement: 1) connection condition of the caisson to SPSP reinforcement; 2) flexural rigidity ratio of caisson to SPSP. A suitable construction method is recommended based on the experimental and analytical results.

1 INTRODUCTION

After the Hyogoken-Nanbu earthquake in Japan, the design codes for highway and railway bridges were revised to meet the needs of much higher strength levels for structures and give social infrastructure higher reliability (Design Codes of Japan Highway Bridges, 2002). In particular, checking of the damage on bridge foundations by earthquake and its reconstruction is more difficult than doing it on bridge piers, it is therefore important to minimize earthquake loss on bridge foundations.

Generally, the best approach is to structurally increase the bearing capacity of the foundation by seismic reinforcement which should be economical and verifiable. In this research, the caisson foundation constructed in water is focused. In reinforcing stiff foundations such as caisson, the increase pile reinforcement is not enough and reinforcement by adding caisson is not reasonable. Therefore, it is thought that SPSP (Steel Pipe Sheet Piles) reinforcement illustrated in Figure 1 in which caisson foundation in water is reinforced by SPSP connected as shown on Figure 2 is suitable for the increasing bearing capacity of existing caisson foundation. SPSP reinforcement method has the following characteristics:

1. Lateral bearing capacity of reinforced foundation system is increased.
2. It can be constructed using short SPSP in a small space under existing bridge in service.
3. It is suitable for reinforcing existing bridge foundation in water.

To design this method economically and accurately, connection condition of the caisson

[i]   Postgraduate, Department of Urban Management, Kyoto University, Japan
[ii] Associate Professor, Department of Urban Management, Kyoto University, Japan
[iii] Professor, Department of Civil Engineering, Nagoya Institute of Technology, Japan
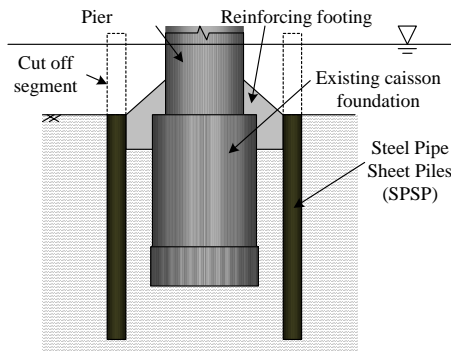[iv] Technical Committee, Japanese Association for Steel Pipe Piles, Japan

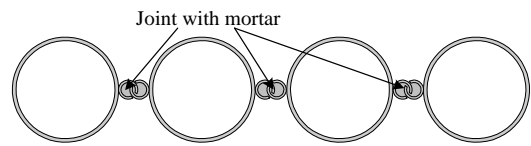Figure 1. Steel Pipe Sheet Pile reinforcement method
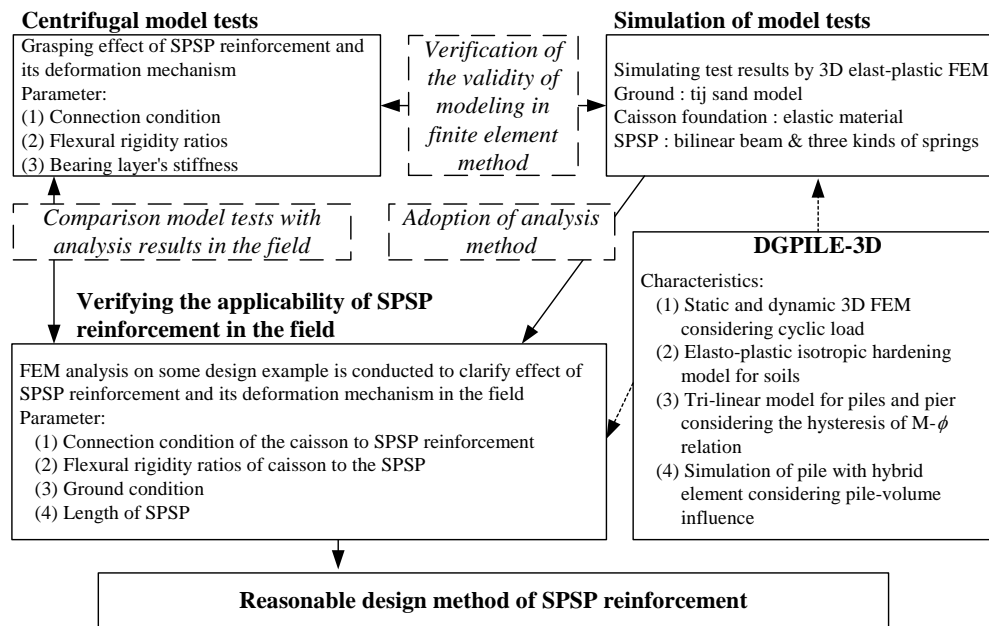

Figure 2. Steel Pipe Sheet Pile

Figure 3. Flow charts of research

to SPSP reinforcement, flexural rigidity ratio of caisson to the SPSP, pile length and distance between caisson and SPSP must be considered adequately. However, the influence of these factors on effect of SPSP reinforcement and its mechanism such as SPSP load ratio, which refers to the total load transmitted from caisson to SPSP reinforcement divided by the total load applied on the SPSP reinforced caisson is not understood. For this reason, the current design method ignores lateral bearing capacity of existing caisson. If this mechanism can be solved, the more rational and economical design method can be proposed.

In this paper, the influence of caisson-SPSP connection condition and flexural rigidity ratio of caisson to SPSP is explained using centrifugal model tests conducted by Isobe and Kimura (2004). Besides, the numerical simulation of the model tests done by Isobe et al. (2005a, 2005b) are showed. 3-D elasto-plastic FEM analysis code: DGPILE-3D (Zhang & Kimura, 2002) is used to simulate the experimental results and the applicability of DGPILE-3D in predicting the mechanical behavior of caisson-SPSP foundation system is verified.

Finally, numerical simulation on a real caisson foundation strengthened using SPSP reinforcement method is conducted and the effect of SPSP reinforcement and its mechanical behavior is discussed. Figure 3 shows a flow chart of the research in this paper and a brief introduction to the code DGPILE-3D. Detailed explanation of the figure will be given in the following sections.

2 CENTRIFUGAL MODEL TESTS

2.1 DETAILED OUTLINE OF CETRIFUGAL MODEL TESTS

Figure 4 shows the experimental apparatus developed by Isobe and Kimura (2004). A model caisson reinforced by the SPSP and embedded in a sandy ground is laterally loaded. The lateral load is applied at a centrifugal acceleration of 50 G on the steel pier fixed on the foundation system after static weight of 200 N is added on the pier to represent dead load of the superstructure. Dry Toyoura sand whose relative density is 89.0 % is used as the pile penetrated layer. A steel block (Young's modulus: 2.0E08 kN/m^2, Poisson's ratio: 0.29) and a lime stabilized block (Young's modulus: 2.6E06 kN/m^2, Poisson's ratio: 0.25) are used as types of the bearing layers. The property and a cross-section of model foundation used in the tests are shown in Table 1 and Figure 5 respectively.

In this research, 20 model test cases are conducted as shown on Table 2. Tests on only caisson are designated Case-1 and tests on caissons reinforced by SPSP are designated Case-2 which are subdivided into Type-A, Type-B and Type-C according to the fixity condition between caisson and SPSP reinforcement. Type-A, Type-B and Type-C, respectively, refers to fixed, just touching and free caisson-SPSP fixity condition. In the case of Type-B, SPSP load ratio is measured by the load cell set between caisson and SPSP. The other details on experiments are described in the reference.

Table 1. Property of the model foundation (Prototype scale)

			Caisson		
SPSP		Type of caisson	S	M	L
Diameter D_p	0.75 m	Diameter D_c		2.5 m	
Length L_p	10.0 m	Length L_c		11.25 m	
Thickness t_p	0.05 m	Thickness t_c	0.05 m	0.25	Solid
No.of Pile	20	Flexural rigidty ratio	0.3	1.2	2.0

Table 2. Test cases

Caisson stiffness	Bearing layer	Caisson (Case-1)	Reinforced caisson system (Case-2)		
			Type-A	Type-B	Type-C
S	Steel	Case-1S$_S$	Case-2AS$_S$	Case-2BS$_S$	Case-2CS$_S$
	Lime	Case-1S$_L$	Case-2AS$_L$	Case-2BS$_L$	Case-2CS$_L$
M	Steel	Case-1M$_S$	Case-2AM$_S$	Case-2BM$_S$	Case-2CM$_S$
	Lime	-	-	-	-
L	Steel	Case-1L$_S$	Case-2AL$_S$	Case-2BL$_S$	Case-2CL$_S$
	Lime	Case-1L$_L$	Case-2AL$_L$	Case-2BL$_L$	Case-2CL$_L$
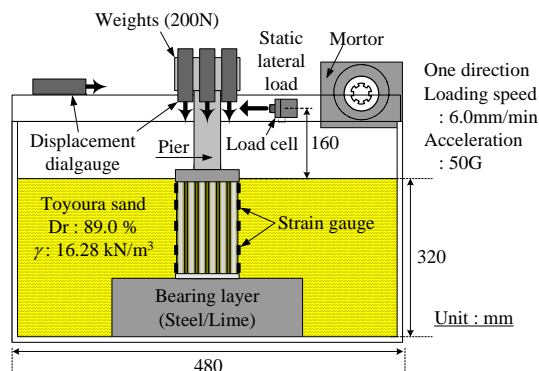
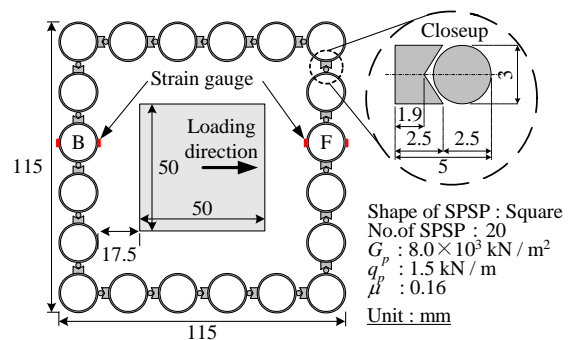Figure 4. A cross-section of test chamber

Figure 5. A cross-section of model foundation

2.2 EXPERIMENTAL RESULTS

In this paper, the influence of caisson-SPSP connection condition and flexural rigidity ratio is explained by comparing the cases hatched in Table 2. Experimental results are converted into prototype scale. Displacement is normalized by caisson diameter. Figure 6 shows effect of SPSP reinforcement for Case-2AL$_L$, Case-2BL$_L$, Case-2CL$_L$, Case-2AS$_L$, Case-2BS$_L$ and Case-2CS$_L$. Effect of SPSP reinforcement is defined as the bearing capacity for Case-2 divided by the bearing capacity for Case-1 at the same displacement. From this figure, the effect of SPSP reinforcement of Case-2AL$_L$ and Case-2AS$_L$ are bigger than 2.5 at a displacement of 5.0%D_c and below. In case of Case-2BL$_L$ and Case-2BS$_L$, the same tendency as Case-2AL$_L$ and Case-2AS$_L$ is seen. However, the reinforcing effect at 5.0%D_c is 1.3. Case-2CL$_L$ and Case-2CS$_L$ have no effect of SPSP reinforcement. Meanwhile, difference in S and L in Type-B and Type-C is not seen, however, S is bigger than L in Type-A.

Figure 7 shows rotation angle for each case at 3.0 MN, load at which rotation angle for Case-1L$_L$ and Case-1S$_L$ increase rapidly. This figure shows that rotation angle of Type-A and Type-B is low, approximately 50% compared with that of Caisson only. However, rotation angle of Type-C is almost the same as that of Case-1L$_L$ and Case-1S$_L$.

SPSP load ratio is defined as the total load transmitted from caisson to SPSP reinforcement wall which is measured by inner load cells divided by the total load applied on the SPSP reinforced caisson system. Figure 8 shows the load ratio-displacement relationship. SPSP load ratio for Case-2BL$_L$ is constantly 40% and Case-2BS$_L$ increases with displacement from 20% to 60%.
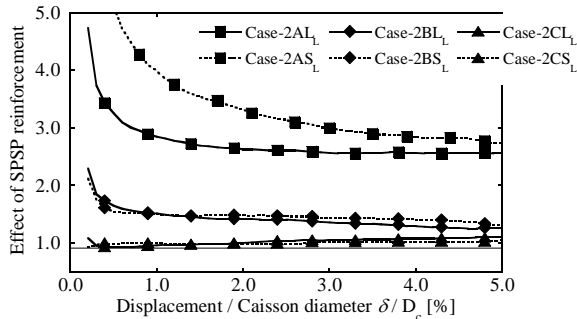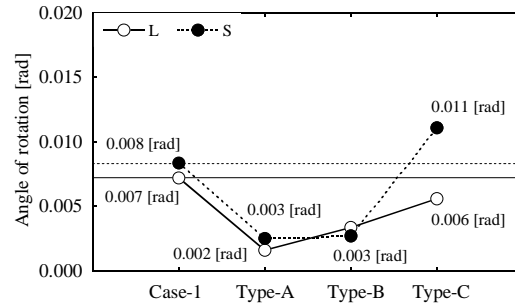

Figure 6. Effect of SPSP reinforcement

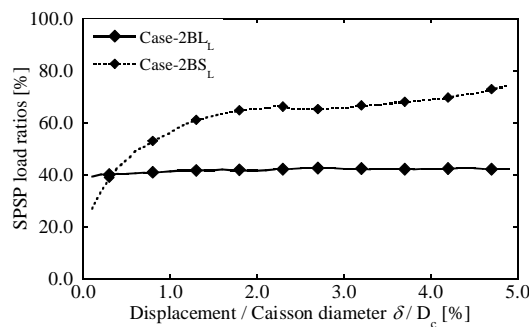Figure 7. Load-rotation angle at applied
load of 3.0 MN

Figure 8. SPSP load ratio-displacement relationship

The following conclusions are obtained from these experiment results. Construction of a footing on the SPSP reinforced caisson to transmit load from the caisson to the SPSP directly is proposed to effectively increase the lateral bearing capacity of the foundation system, however, it may not be necessary to use a completely fixed footing (as Type-A), Type-B condition will suffice. When the flexural rigidity ratio is larger than 1.0 like it is in S, the reinforcement is considered to be effective.

3 NUMERICAL SIMULATION OF MODEL TESTS

In this research, numerical simulation of centrifugal model test results is conducted using 3D Elasto-Plastic FEM Analysis code: DGPILE-3D by Isobe et al. (2005a, 2005b). By comparing the experimental results with simulation results, it is verified that it is possible to adopt DGPILE-3D to predict the mechanical behavior of SPSP reinforcement caisson foundation systems subjected to lateral loading.

In order to properly evaluate mechanical behaviors of SPSP reinforced caisson foundation, constitutive models for soil skeleton play a very important rule in numerical analyses. In present research, tij sand model (Nakai, 1986) were used for dense density dry Toyoura sand in finite element analyses, in which the influence of the intermediate principal stress can be properly evaluated. The model has been verified through many true triaxial tests on normally consolidated sand in generalized stress paths. The parameters involved in the tij models are almost the same as those in Cam-clay model. Therefore, it is rather easy to determine the values of these parameters with conventional triaxial compression and consolidation tests. Figure 9 shows the comparison of theoretical and the test results of stress-strain-dilatancy relations in different stress paths obtained from true triaxial tests on Toyoura sand. Seven parameters are involved in tij sand model, namely compression index λ, swelling index κ, Poisson's ratio ν, gradient parameter of stress-dilatancy relation α (In Cam-clay model, $\alpha = 1$), stress ratio at critical state Rf, exponential expression of stiffness of sand in elastic region m and gradient parameter of stress-dilatancy relation in swelling process of sand Df. All these parameters can be easily determined by conventional triaxial compression tests and its detailed description can be referred to in the reference.

The bearing layers made from steel and lime stabilized sand modeled as an elastic solid element. In this simulation, a very thin layer modeled by tij sand model is used to simulate the rotation behavior of the caisson. And the parameters of this thin layer are determined to be as close as possible as those of centrifugal test results of Case-1L_L as shown in Figure 10.

The caisson foundation is modeled as elastic material and the SPSP is described using bilinear beam with three different kinds of springs, which indicate horizontal resistance and vertical shearing resistance of SPSP joint. The two horizontal springs (in x and y direction) are linear and one vertical spring (in z direction) is bilinear. The nonlinearity of the pile is calculated according to Design Codes of Japan Highway (2002). The nonlinearity of spring modelling SPSP joints: G_p and q_p is determined by joint shearing test.

The parameters used in the finite element analysis are listed in Tables 1 and 3, Figure 5.

The detailed of the numerical simulation is described in the reference.

Figure 10 shows the experiment and simulation results on load-displacement relationship and load-rotation angle for Case-1L$_L$ and Case-2AL$_L$. The analysis result can express the experiment result with a certain amount of accuracy. For this reason, it is possible to predict the mechanical behavior of the caisson foundation reinforced by SPSP in terms of load-displacement and load-rotation angle relationship.

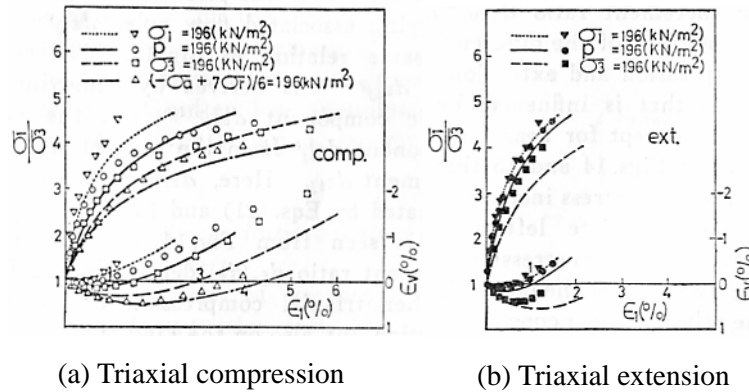(a) Triaxial compression

(b) Triaxial extension

Figure 9. Simulation of stress-strain-dilatancy relation of Toyoura Standard sand under different stress paths with tij sand Model (Nakai, 1989)

Table 3. Material parameters of the model ground

	Thickness H	Density ρ	Innertia friction angle ϕ	Young's modulas E	Poisson's ratio ν	Compression cofficient C_i
	[m]	[g/cm³]	[°]	[kN/m²]	-	-
Pile penetrated layer	10.25	1.596	(36.8)	—	0.30	0.0084
Thin layer	0.25	1.596	(36.8)	—	0.30	0.000215
Bearing layer	5.5	0.810	—	2.6×10^6	0.25	—

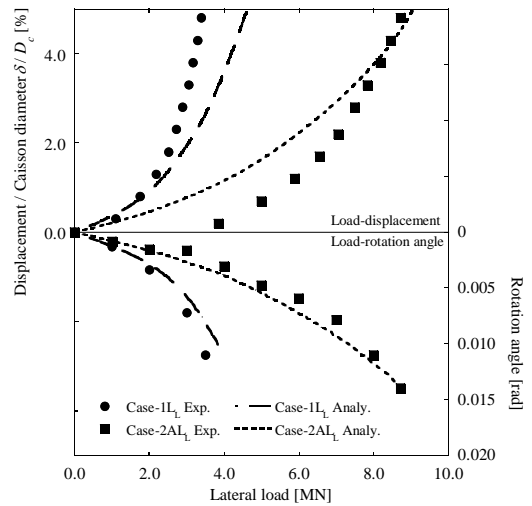|	Swelling cofficient C_e	Stress ratio at critical state R_f	Initial void ratio e_0	gradient parameter of Stress-dilatancy relation α	gradient parameter of Stress-dilatancy relation in swelling process D_f
	-	-	-	-	-
Pile penetrated layer	0.0060	4.0	0.66	0.85	-0.6
Thin layer	0.000135	4.0	0.66	0.85	-0.6
Bearing layer	—	—	—	—	—

Figure 10. Comparison of load-displacement and load-rotation angle relationship observed from the experiment with the simulation

4 NUMERICAL SIMULATION OF MECHANICAL BEHAVIOR OF A REAL SPSP REINFOCED CAISSON

4.1 DETAILED OUTLINE OF A PRACTICAL SAMPLE

In order to verify practicability of SPSP reinforcement method on existing caisson, numerical simulation on a practical sample of SPSP reinforced caisson is conducted using DGPILE-3D.

The sample is an oval-shaped caisson foundation, 10.5 m in length, 5.5 m in width and 15.0 m in depth reinforced by 38 SPSP which were 800.0 mm in diameter and 15.0 m in depth. In the simulation, the caisson is modeled as rectangular shape which has (Length x Width x Depth) of 4.4 x 9.4 x 15.0 m as shown in Figures 11 and 12. In modeling caisson like this, the distance between caisson and SPSP, the effective width on which subgrade reaction is obtained is considered. However, flexural rigidity of caisson and SPSP in numerical simulation is equivalent to that of original caisson and SPSP by changing young's modulus of elastic solid elements and beam elements which model caisson and SPSP. Flexural rigidity ratio of caisson to SPSP in the sample is 1.46.
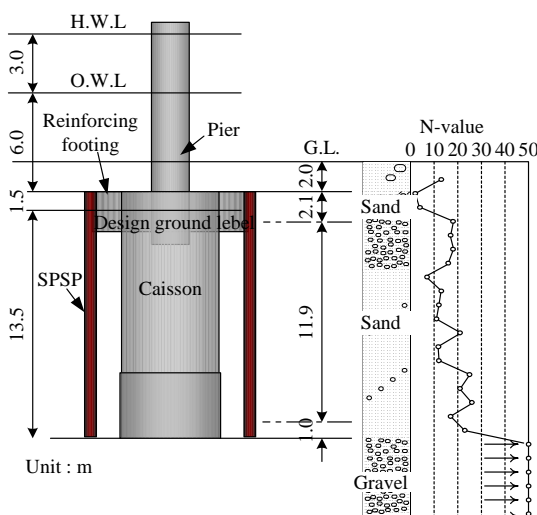

Figure 11. A cross-section of SPSP reinforced caisson foundation system and ground condition
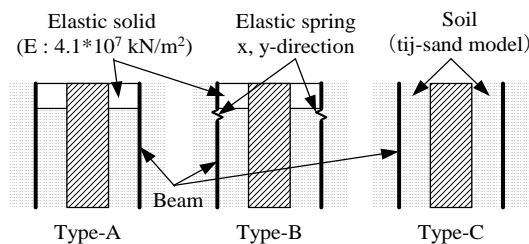

Figure 12. Modeling of caisson foundation

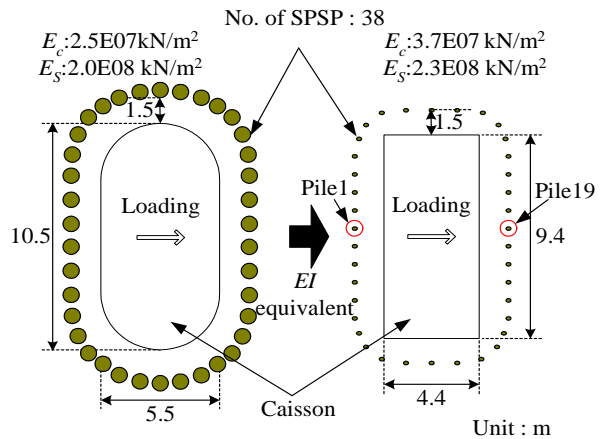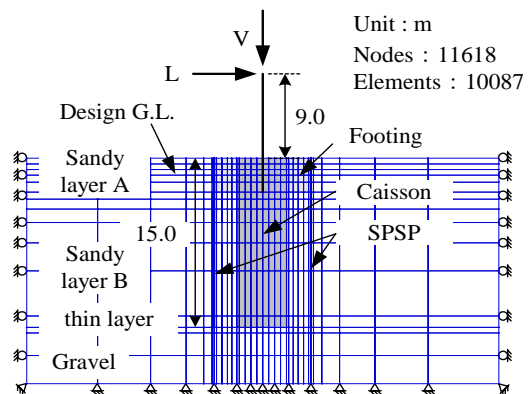Figure 13. Modeling of connection condition on footing

Figure 14. Configuration of SPSP reinforced caisson foundation and finite element mesh

Also in this simulation, the influence of the footing connection condition on effect of SPSP reinforcement and its deformation behavior is discussed to propose more reasonable reinforcement method. Footing condition is divided into Type-A (fixed), Type-B (lateral load only transmitted) and Type-C (no footing) like in the experiment. The footing is modeled as shown in Figure 13. In a modeling footing of Type-B, the elastic springs are used instead of the beam element right under footing to transmit neither moment nor axial force to SPSP. The footing thickness is 3.0 m.

The ground is modeled by tij sand model. A very thin layer modeled by tij sand model is used to simulate the rotation behavior of the caisson. The parameters of the soil model used in the finite element analyses are shown in Table 4.

The caisson foundation is modeled as elastic material and the SPSP is described using bilinear beam with two different springs which model the SPSP joints just like in the simulation of experiment model tests. The nonlinearity of pile and spring of SPSP is calculated according to Design Codes of Japan Highway (2002). The properties of the foundation are also shown in Figures 11 and 12.

By considering symmetry, geometrical and loading conditions, only half of the domain is used in the analysis. The finite element mesh is prepared as shown in Figure 14. The boundary conditions are: (a) the bottom of the ground is fixed; (b) the vertical boundaries parallel to the XOZ plane are fixed in the y direction and free in the x and z directions; (c) the vertical boundaries parallel to the YOZ plane are fixed in the x direction and free in the y and z directions. These calculations are conducted under drained condition, that is, the pore water pressure is not considered. In this research, five cases are calculated: caisson, SPSP and three types of SPSP reinforced caisson designated Caisson, SP and Type-A, Type-B, Type-C respectively. Analysis cases are shown in Figure 15.

A prescribed incremental load is applied in one direction, and the vertical loading (Caisson, SP, Type-A, Type-B, Type-C; 20.9 MN; 18.4 MN) and the lateral loading (Caisson; 8.0 MN, SP, Type-A, Type-B and Type-C; 12.0 MN) are divided into 20 steps and 20 steps respectively. That is, the required SPSP reinforcement effect of lateral bearing capacity in the sample is 1.5 (= 12.0 MN / 8.0 MN).

4.2 ANALYTICAL RESULTS

Figure 16 shows load-displacement relation and Figure 17 shows effect of SPSP reinforcement. As the figures indicate, effect of SPSP reinforcement of Type-A and Type-B decrease with an increase in displacement. These values are converged to 1.9 and 1.6, respectively, however, meet required increase magnification of lateral bearing capacity; 1.5. On another front, effect of SPSP reinforcement of Type-C is almost near 1.0. It should also be added that displacement of Type-C under lateral bearing capacity load required for reinforced caisson foundation system becomes bigger than that of Caisson.

Load-rotation angle relation and effect of SPSP reinforcement for rotation angle appear in Figures 18 and 19. In these figures, it has been found that Type-A and Type-B is effective, Type-C has no effectiveness.

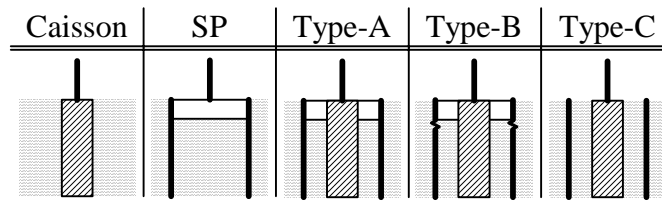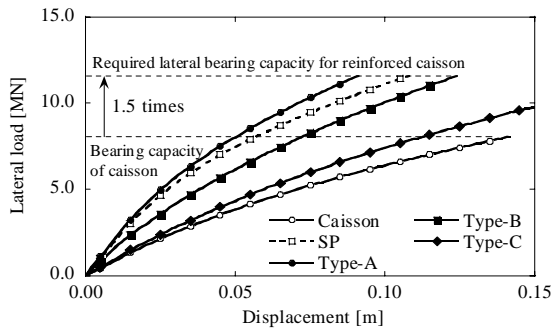| Caisson	SP	Type-A	Type-B	Type-C

Figure 15. Analysis cases
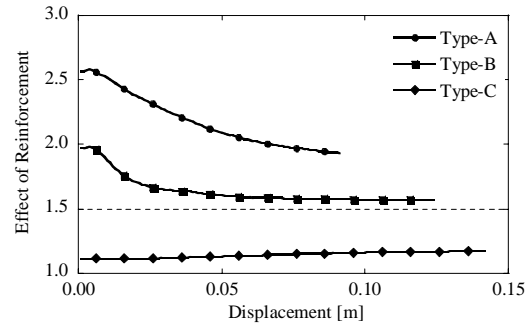
Figure 16. Load-Displacement relation
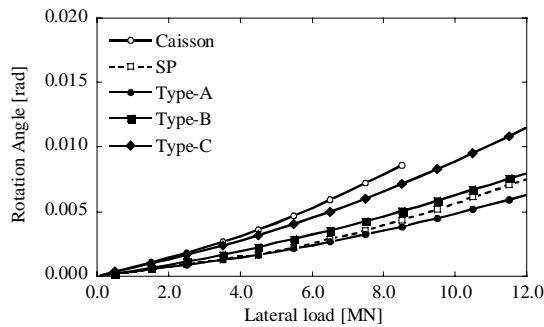at loading point

Figure 17. Effect of SPSP reinforcement
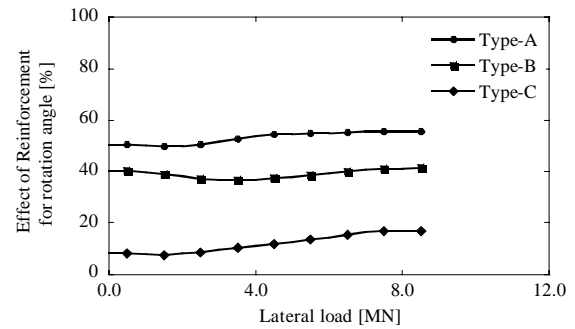
Figure 18. Load-Rotaion angle relation

Figure 19. Effect of SPSP reinforcement
for rotation angle

Figure 20 shows SPSP load ratio, which refers to the total load transmitted from caisson to SPSP reinforcement divided by the total load applied on the SPSP reinforced caisson. In this figure, x axis indicates the applied lateral load and y axis the total shear force in all piles. The validity of this evaluation method concerning SPSP load ratio is proven by the result that the total shear force in all piles is equal to the applied lateral load in SP. SPSP load ratio of Type-B and Type-C are almost 50% and less than 10%, respectively. Meanwhile, SPSP load ratio of Type-A is approximately 50%, increases gradually and reaches up to 70% in 5MN or more. ****

As mentioned above, it turns out that the seismic reinforcement in Type-A and Type-B also demonstrates the reinforcement effectiveness and the reduction effect of rotation angle, and that connection condition between caisson and SPSP influences SPSP load ratio greatly.

Table 4. Material parameters of the ground

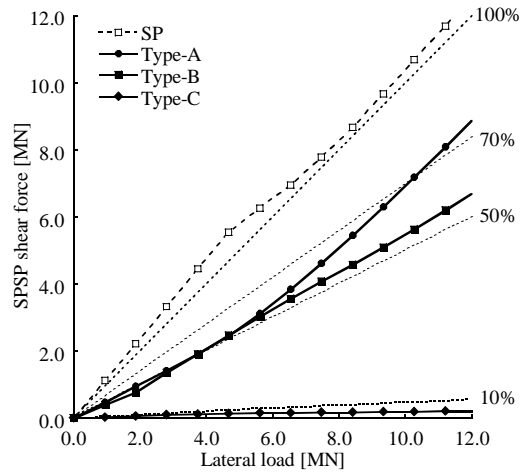|	Thickness H	Density ρ	Innertia friction angle ϕ	Young's modulas E	Poisson's ratio ν	Compression cofficient C_t
	[m]	[g/cm³]	[°]	[kN/m²]	-	-
Sandy layer A	0.6	1.8	(30.0)	—	0.33	0.04
Sandy layer B	11.9	1.8	(30.0)	—	0.33	0.009
Thin layer	0.5	2.0	(36.8)	—	0.33	0.04
Bearing layer	4.5	2.0	(36.8)	—	0.33	0.0025
	Swelling cofficient C_e	Stress ratio at critical state R_f	Initial void ratio e_0	gradient parameter of Stress-dilatancy relation α	gradient parameter of Stress-dilatancy relation in swelling process D_f
	-	-	-	-	-
Sandy layer A	0.02	3.05	0.89	0.85	-0.6
Sandy layer B	0.0029	3.05	0.89	0.85	-0.6
Thin layer	0.002	4.7	0.61	0.85	-0.6
Bearing layer	0.0012	4.7	0.61	0.85	-0.6

Figure 20. SPSP load ratio

Figure 21 and Figure 22 show bending moment, axial force distribution and lateral displacement on SPSP marked in Figure 12 at a load of 12.0MN. In this figure concerning axial force distribution, positive value and negative value, respectively, refers to compressive force and tensile force.

Type-B generates the biggest bending moment in SPSP reinforced caisson, the moment on Pile1 and Pile19 in Type-A is suppressed to about the half of the moment in SP. The moment distribution on Pile1 and Pile19 in Type-C is greatly different from that in the other cases. It can be seen that there is no difference in moment distribution on Pile1 and Pile19 in each case. The reason is that all piles are connected by springs in the calculation, and SPSP reinforcement, that is, all piles move together. The deformation mechanism is different from the experimental result; however, it is thought that an analytical results show more actual deformation mechanism than the experimental results.

On the contrary, axial force distribution on Pile1 and Pile19 are quite different in each case. Especially, it is remarkable in Type-A and SP. In both cases, compressive force is generated in Pile19, and tensile force is generated in Pile1. Though tensile force generated on pile1 in Type-A and SP doesn't have the enormous discrepancy, compressive force generated on pile19 is greatly different in Type-A and SP. In a word, the maximum value of Type-A becomes about 2/3 of the maximum values of SP and the load concerning compressive force of Type-A is smaller than that of SP. From the result the axial force on piles in Type-B and Type-C is almost near zero. It has been found that the reinforcement effect is not demonstrated by axial force of SPSP in Type-B, the reinforcement effect is not obtained in Type-C.

From these results, it is observed that the reinforcement effect is demonstrated by only bending deflection of SPSP in Type-B, and that the reinforcement effect is demonstrated by resisting lateral load by both bending deflection and axial force of SPSP (compressive force and tensile force on piles) in Type-A.

Furthermore, effective reinforcement is expected from the reinforcement connection system of Type-B although the reinforcement effect is a little smaller than when Type-A connection is used. Meanwhile, there is a trial calculation that 20 % - 40 % of construction
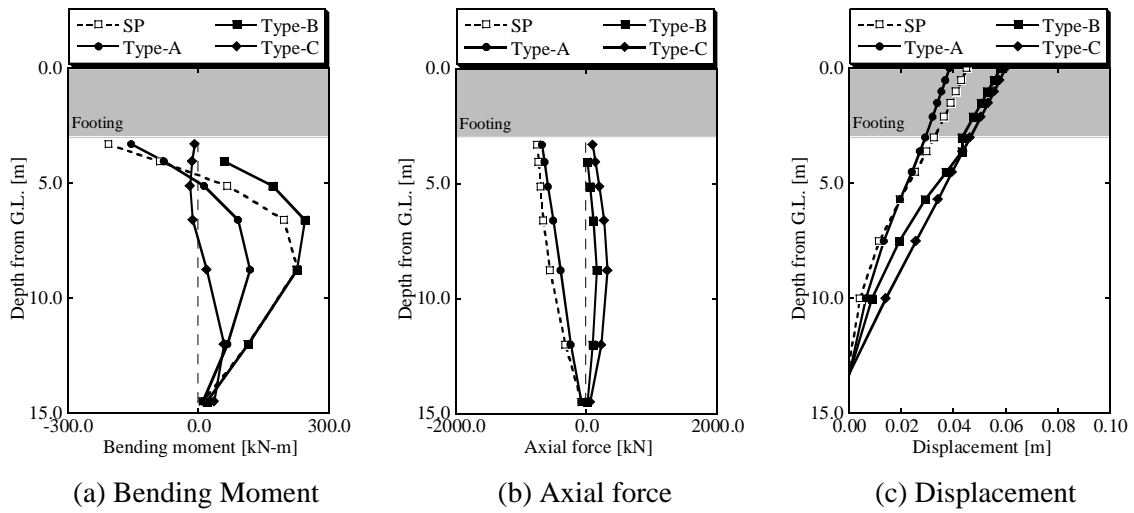
(a) Bending Moment   (b) Axial force   (c) Displacement

Figure 21. Sectional force of Pile1

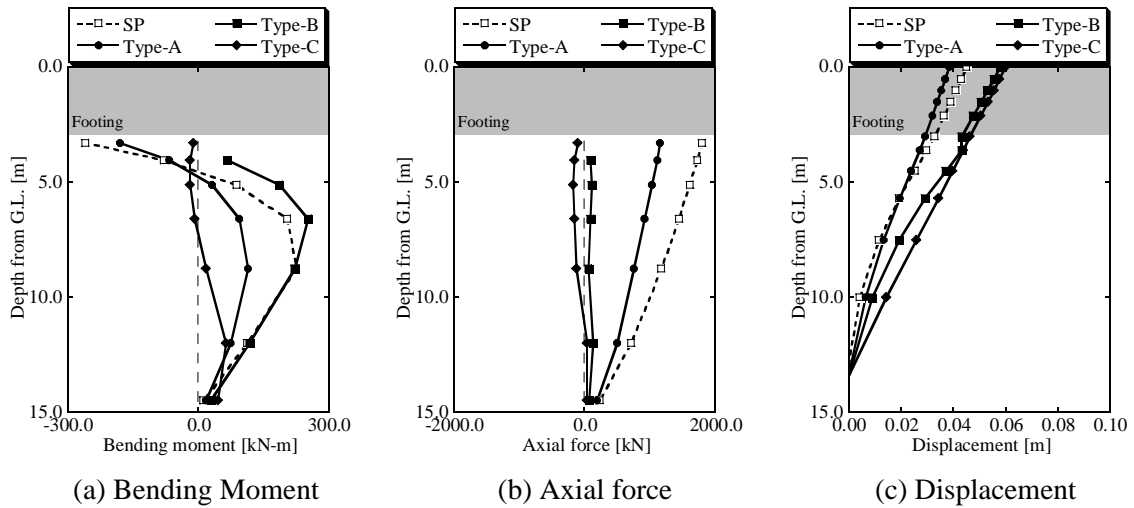(a) Bending Moment   (b) Axial force   (c) Displacement

Figure 22. Sectional force of Pile19

cost can be reduced by applying Type-B compared with current construction (Type-A). Therefore, more economical and more reasonable reinforcement method like Type-B is recommended.

5 CONCLUSIONS

Reinforcement effect and its physical mechanism of existing caisson foundation reinforced by SPSP are verified by centrifugal model tests and numerical simulation, the following conclusions were made:

1. Influence of connection condition between caisson and SPSP on reinforcement effect is significant.
2. Since SPSP load ratio is influenced by flexural rigidity ratio, the establishment of a design method which puts into consideration flexural rigidity ratio is required.
3. Footing condition of Type-B meets the required lateral bearing capacity requirements

of an SPSP reinforced caisson foundation.
4. Design method for SPSP reinforced caisson, in which load distribution between caisson and SPSP is considered, is necessary.
5. It is possible to simulate the mechanical behaviour of SPSP reinforced caisson foundation and estimate the effect of SPSP reinforcement on Caisson foundation by using DGPILE-3D.

6 REFFERENCES

1) Japan Road Association 2002. Design Codes of Japan Highway, ISBN 4-88950-247-5 C2051, Maruzen Print Co. Ltd., (in Japanese).
2) Isobe, K. and Kimura, M. 2004. Centrifugal model tests on effect of steel pipe sheet pile reinforcement on existing caisson foundation, *The Seventeenth KKCNN Symposium on Civil Engineering*, 463-468.
3) Isobe, K., Kimura, M., Yoshizawa, Y., Kohono, K., Harata, N. and Makino, T. 2005. Evaluation of effect of strengthening existing caisson foundation against earthquake by steel pipe sheet piles using 3D elasto-plastic FEM analysis, *Proc.11th Int. Conf. of IACMAG* , No.2, 459-466.
4) Isobe, K. and Kimura, M. 2005. Mecahnical behavior of caisson foundation reinforced by steel pipe sheet piles, *16th International Conference on Soil Mechanics and Geotechnical Engineering*, 1493-1496.
5) Nakai, T. 1989. An isotropic hardening elasto-plastic model for sand considering the stress path dependency in three-dimensional stresses, *Soils and Foundations*, Vol.29, No.1, 119-137.
6) Zhang, F. and Kimura, M. 2002. Numerical Prediction of the Dynamic Behaviors of an RC Group-file Foundation, *Soils and Foundations*, Vol.42, No.3, 77-92.